Article

Discovery Medicine 2024; 36(187): 1678–1691
https://doi.org/10.24976/Discov.Med.202436187.154

Targeting STIM1 Contributes to Alleviating Remodeling of Vascular Smooth Muscle Cells in Atherosclerosis

Zhenyu Cui[1,†], Yue Zhang[1,†], Lezhi Sheng[1,*]

[1]Department of Cardiovascular Medicine, Shanghai Pudong New Area People's Hospital, 201299 Shanghai, China
*Correspondence: shenglezhi_shlz@163.com (Lezhi Sheng)
†These authors contributed equally.
Published: 20 August 2024

Background: Remodeling of vascular smooth muscle cells (VSMCs), as a pathological hallmark of cardiovascular diseases, is related to the molecular rewiring of Calcium signaling, which induces upregulation of stromal interaction molecule (STIM) proteins. This study analyzed the influence of STIM1 proteins on the remodeling of VSMCs in atherosclerosis (AS).
Methods: After oxidized low-density lipoprotein (ox-LDL) treatment and transfection, VSMC viability, migration, and invasion were separately measured using Cell Counting Kit-8, Scratch assay, and Transwell assay. An animal AS model was constructed, and histological analysis via hematoxylin-eosin staining was conducted on the aorta.
Results: Ox-LDL promoted expression of STIM1 and Orai calcium release-activated calcium modulator 1 (Orai1). STIM1 or Orai1 downregulation suppressed viability, migration, invasion, and phenotypic switching of ox-LDL-treated VSMCs, whereas STIM1 or Orai1 upregulation had opposite effects. Orai1 level was upregulated by STIM1 overexpression. Orai1 silencing reversed the effects of STIM1 overexpression in VSMCs. STIM1 deficiency alleviated AS and regulated expression of Orai1 and phenotypic switch-related factors *in vivo*.
Conclusion: STIM1 deficiency suppresses viability, migration, invasion, and phenotypic switching of ox-LDL-induced VSMCs and alleviates AS by inhibiting Orai1.

Keywords: atherosclerosis; stromal interaction molecule 1; Orai calcium release-activated calcium modulator 1; vascular smooth muscle cells

Introduction

The majority of cardiovascular diseases (CVDs) are primarily attributable to atherosclerosis (AS), a condition that is not only considered a leading threat to global health but also carries a heavy social burden. Ischemic heart disease and stroke caused by AS are the world's largest killers, causing more than 15 million deaths every year [1,2]. In 2019, approximately 17.9 million people succumbed to CVDs globally, constituting 32% of the total global deaths [3]; in China, CVD was the leading cause of death among residents, accounting for 46.66% of mortality in rural areas and 43.81% in cities [3]. In the process of AS progression, myeloid cells may destabilize plaques within the arterial wall and cause them to rupture, which can trigger myocardial infarction and stroke [4]. Conversely, acute myocardial infarction (AMI) has been suggested to aggravate atherosclerotic lesions by accelerating their growth and/or promoting plaque instability [5]. Currently, despite the introduction of physical or pharmacological methods for preventing the formation of AS and thrombus, the incidence of advanced AS-associated clinical adverse events remains high. Therefore, it is critical to continue developing a feasible and efficient therapeutic approach for the prevention and treatment of AS [6].

Vascular smooth muscle cells (VSMCs) are the major cell type in all stages of an atherosclerotic plaque; these highly specialized cells are responsible for vessel homeostasis and blood pressure control, and exhibit a contractile phenotype once matured and fully differentiated [7,8]. Remodeling of VSMCs, as a pathological hallmark of CVDs, is related to the molecular rewiring of Calcium (Ca^{2+}) signaling, which induces upregulation of stromal interaction molecule (STIM) proteins [9]. STIM- and Orai calcium release-activated calcium modulator (Orai) proteins-mediated store-operated Ca^{2+} entry (SOCE) has been suggested as a highly regulated and ubiquitous signaling pathway, which exerts significant effects in a variety of both cellular and physiological functions, including vascular disorders [10]. STIM1 is one of the endoplasmic reticulum (ER) membrane proteins activated as a consequence of ER Ca^{2+} concentration reduction [11]. STIM1 deficiency can promote the viability and migration of VSMCs [12].

Reportedly, STIM1 regulates Ca^{2+} signaling by activating Orai calcium release-activated calcium modulator 1 (Orai1), which is a Ca^{2+} channel [13,14]. Importantly, the upregulation of Orai1 has been proven to increase Ca^{2+} and contribute to Angiotensin II (Ang II)-induced VSMC proliferation [15]. Moreover, a recent review considered

Orai1-driven SOCE as a therapeutic target in pathological vascular remodeling [16]. However, the interaction between STIM1 and Orai1 in AS has not been reported. Oxidized low-density lipoprotein (ox-LDL) is instrumental in AS and is used for AS modeling *in vitro* [17]. Hence, the purpose of this research is to determine the functions and impacts of Orai1 and STIM1 in AS. In this study, we used an Apolipoprotein E-deficient ($ApoE^{-/-}$) AS mouse model to observe the changes in STIM1 expression in aortic VSMCs during the formation of atherosclerotic plaques, to clarify its relationship with the occurrence and development of atherosclerotic plaques, and to provide novel insights for AS prevention and treatment.

Materials and Methods

Cell Culture and Treatment

Mouse aortic VSMCs (MOVAS-1, AW-CELLS-M0118) were provided by AnWei-sci (Shanghai, China) and seeded in Dulbecco's modified eagle's medium (DMEM, PM150223A, Pricella, Wuhan, China) with 10% fetal bovine serum (FBS, AW-FBS-001, AnWei-sci, China) and 0.2 mg/mL G418 (A1720, Sigma-Aldrich, St Louis, MO, USA). The incubation was completed in 96-well plates in an incubator (37 °C, 5% CO_2). In addition, VSMCs routinely underwent mycoplasma contamination testing and were mycoplasma-free. 50 ng/mL ox-LDL (L34357, Invitrogen, Carlsbad, CA, USA) was used to treat VSMCs for 24 h [18].

Immunofluorescence Assay

VSMCs were fixed with 4% paraformaldehyde (abs9179, Absin, Shanghai, China) for 15 min and permeabilized with 0.1% Triton X-100 (abs47048168, Absin, China) for 10 min at room temperature, followed by PBS washing and 30 min incubation with 5% bovine serum protein (ST2254, Beyotime, Shanghai, China) at 37 °C. Primary antibody against α-smooth muscle actin (α-SMA) (14-9760-95, Thermo Fisher, Waltham, MA, USA) was used to incubate the cells at 4 °C overnight, and incubation with fluorescence-labeled secondary antibody (A-10667, Thermo Fisher, USA) was performed for 30 min at 4 °C. Thereafter, cell nuclei were stained with 2-(4-amidinophenyl)-6-indolecarbamidine dihydrochloride (C1005, Beyotime, China) for 10 min away from light. A confocal microscope (FV3000, Olympus, Tokyo, Japan) was employed to observe the stained cells under $\times$200 magnification.

Transfection

Short hairpin RNA (shRNA) targeting *STIM1* (shSTIM1, C02001, 5′-CCCTTCCTTTCTTTGCAATAT-3′) and negative control shRNA (shNC, C02001, 5′-CCTAAGGTTAAGTCGCCCTCG-3′) were procured from GenePharma (Shanghai, China). Small interfering RNA (siRNA) targeting *Orai1* (siOrai1, stB0003521A-1-5, 5′-CACACTTGTATGTACACATAA-3′) and siRNA for negative control (siNC, siN0000002-1-5, 5′-CAACAAGATGAAGAGCACCAA-3′) were additionally purchased from RiboBio (Guangzhou, China). Overexpression plasmids were obtained by insertion of coding sequence (CDS) regions of *STIM1* and *Orai1* into pcDNA3.1(+) vector (VT1001, YouBio, Changsha, China). When the confluence of VSMCs (1×10^6 cells/well) in 6-well plates reached 90%, liposome complexes of the above vectors were prepared using Lipofectamine 3000 Reagent (L3000001, Invitrogen, USA) to incubate cells (48 h, 37 °C) for transfection.

Cell Counting Kit-8 (CCK-8) Assay

Next, treated/transfected VSMCs (5×10^3 cells/well) were grown in 96-well plates (37 °C, 5% CO_2, 24/48 h) and cultivated with 10 µL/well CCK-8 reagent (CA1210, Solarbio, Beijing, China) (37 °C, 4 h). Detection of optical density (OD) value (450 nm) was performed employing a Multiskan™ FC Microplate Photometer (51119180ET, Invitrogen, USA).

Scratch Assay

Transfected/treated VSMCs (1×10^5 cells/well) were plated in 6-well plates, and an artificial scratch was made using a sterile pipette tip on the cell monolayer with approximately 80% confluence. After culturing cells in serum-free medium (37 °C, 5% CO_2), images (0/24 h) were acquired utilizing an Eclipse Motic AE2000 inverted optical microscope ($\times$100 magnification, Microscope Central, Feasterville, PA, USA). The cell migration rate = (scratch width at 0 h – scratch width at 24 h)/scratch width at 0 h $\times$ 100%, followed by normalization of data in other groups to those of the control group.

Transwell Assay

VSMCs (1×10^4 cells/well) suspended in a serum-deprived medium (100 µL) were added to the matrigel (E1270, Sigma-Aldrich, USA)-precoated upper chamber of 6-well Transwell plates (8-µm pore filters, 140644, Invitrogen, USA), with the lower chamber full of 600 µL normal medium containing 10%–20% FBS. Following 24-h cultivation in an incubator, only cells in the lower chamber experienced 30-min fixation (4% paraformaldehyde, abs9179, Absin, China) (room temperature (RT)) and staining in Giemsa (abs47047618, Absin, China). Finally, cells were observed under an Eclipse Motic AE2000 inverted optical microscope ($\times$250 magnification) to obtain the invasion rate ([the number of observed cells/total cell number] $\times$100%), and the data in other groups were normalized to those in the control group.

Animal Model

In accordance with a previous study, an AS animal model was constructed [19]. Briefly, male ApoE$^{-/-}$ C57BL/6J mice (7–8 weeks old, 20 ± 2 g, n = 40) were kept in standard specific pathogen-free (SPF) cages (12-h day/light cycle, 22–24 °C, 50–60% humidity). Following a week of adaptive feeding with a standard experimental diet, all mice were randomized into Control, Model (AS), Model+shNC, and Model+shSTIM1 groups (n = 10/group). Except for those in the Control group, mice continued to be fed using a high-fat diet containing 1.25% cholesterol, 15% fat, and sterile water to construct the AS model [20].

Adeno-associated virus (AAV) carrying shNC or shSTIM1 was purchased from GenePharma (China). After high-fat diet feeding for 12 weeks, mice in the Control and Model groups only received tail vein injection of an equivalent volume of saline (PB180353, Pricella, China), whereas those in the Model+shNC and Model+shSTIM1 groups received tail vein injection of AAV-shNC and AAV-shSTIM1, respectively, for 3 successive days, and high-fat diet for additional 3 weeks. Then, all mice were sacrificed via inhalation of 5% isoflurane (792632, Sigma-Aldrich, USA) and cervical dislocation. The left ventricle was then perfused using phosphate buffer saline (PBS, P301981, Aladdin, Shanghai, China) to remove excessive blood. The aorta sample was immediately resected, and fixed in 4% paraformaldehyde (C104190, Aladdin, China) or placed in a –80 °C refrigerator. Aortic atheromatous plaque formation and reduced VSMCs indicated the success of model construction, with the success rate of model construction of 90%.

Hematoxylin-Eosin (H&E) Staining

After 48-h fixation, aorta tissues were dehydrated and permeabilized using alcohol (51976, Sigma-Aldrich, USA) and xylene (XX0060, Sigma-Aldrich, USA). 6-µm aorta sections were created following paraffin embedding, deparaffinized in xylene and rehydrated with graded ethanol, after which staining with H&E (H3136; 861006, Sigma-Aldrich, USA) was conducted for 5 min and 3 min (RT), in sequence. All samples were observed and analyzed using an Eclipse Motic AE2000 inverted optical microscope (×200 magnification).

Immunohistochemistry (IHC) Analysis

Aorta slides were reacted with citrate buffer (PH. 6.0, C2488, Sigma-Aldrich, USA) (100 °C, 7 min) for antigen retrieval, then blocked with 5% goat serum (C1771, Applygen, Beijing, China) for 1 h. All paraffin-embedded sections were stained using antibodies (Abcam, Cambridge, UK) STIM1 (ab108994, 1:100) (4 °C, overnight) and Goat Anti-Rabbit immunoglobulin G (IgG) heavy and light chains (H&L) (ab205718, 1:5000), and visualized with a 3,3′-Diaminobenzidine (DAB) kit (95041-478, VWR, Radnor, PA, USA) (15 min, RT). After final staining with hematoxylin, STIM1-positive cells were counted in five random areas and observed under a stereo microscope (×200 magnification, SZX7, Olympus, Japan).

RNA Isolation and Quantitative Real-Time Polymerase Chain Reaction (qRT-PCR)

Total RNA was procured using a TRIzol™ Plus RNA Purification Kit (12183555, Invitrogen, USA) from treated or transfected VSMCs, and the complementary DNA (cDNA) creation was achieved using a SuperScript™ VILO™ cDNA Synthesis Kit (11754050, Invitrogen, USA). Afterwards, the cDNA and primers were applied for qRT-PCR with Fast SYBR™ Green Master Mix (4385612, Invitrogen, USA) in a QuantStudio™ 7 Pro real-time PCR instrument (A43165, Invitrogen, USA), with the following conditions: 95 °C (20 sec), 40 cycles at 95 °C (3 sec), and 60 °C (30 sec). Finally, all data were processed using the $2^{-\Delta\Delta CT}$ method [21], with β-actin as loading control. Table 1 lists the primer sequences used.

Table 1. Primers for qRT-PCR.

Gene	Primers (5′->3′)
STIM1 (mouse)	
F	ATGGATGAGGAGATTGTGT
R	CAAATCCCTCTGAGATCC
α-SMA (mouse)	
F	ACGAATTTGCGTGTCATCCT
R	AGACAGAGTACTTGCGTTCT
SM22α (mouse)	
F	AAGAATGGTGTGATTCTGAG
R	GCCATATCCTTACCTTCATA
VEGF (mouse)	
F	GGATTATGTCAGAAAAGGAG
R	GTACATTTCTGGGGTAGTGT
MMP-9 (mouse)	
F	CCCACTTACTATGGAAACTC
R	CTTATCGTAGTCAGCTGTTG
β-actin (mouse)	
F	CTATGTTGCTCTAGACTTCG
R	ATAGAGGTCTTTACGGATGTC

STIM1, stromal interaction molecule 1; *α-SMA*, α-smooth muscle actin; *SM22α*, smooth muscle protein-22α; *VEGF*, vascular endothelial growth factor; *MMP-9*, matrix metalloproteinase-9; F, forward; R, reverse; qRT-PCR, quantitative real-time polymerase chain reaction.

Western Blotting

Proteins were extracted from treated or transfected VSMCs using Radioimmunoprecipitation assay (RIPA) Buffer (R0010, Solarbio, China) and a mixture of protease and phosphatase inhibitor (P1261, Solarbio, China), followed by a 5-min boiling water bath. Protein concentration measurement was completed using a bicinchoninic acid

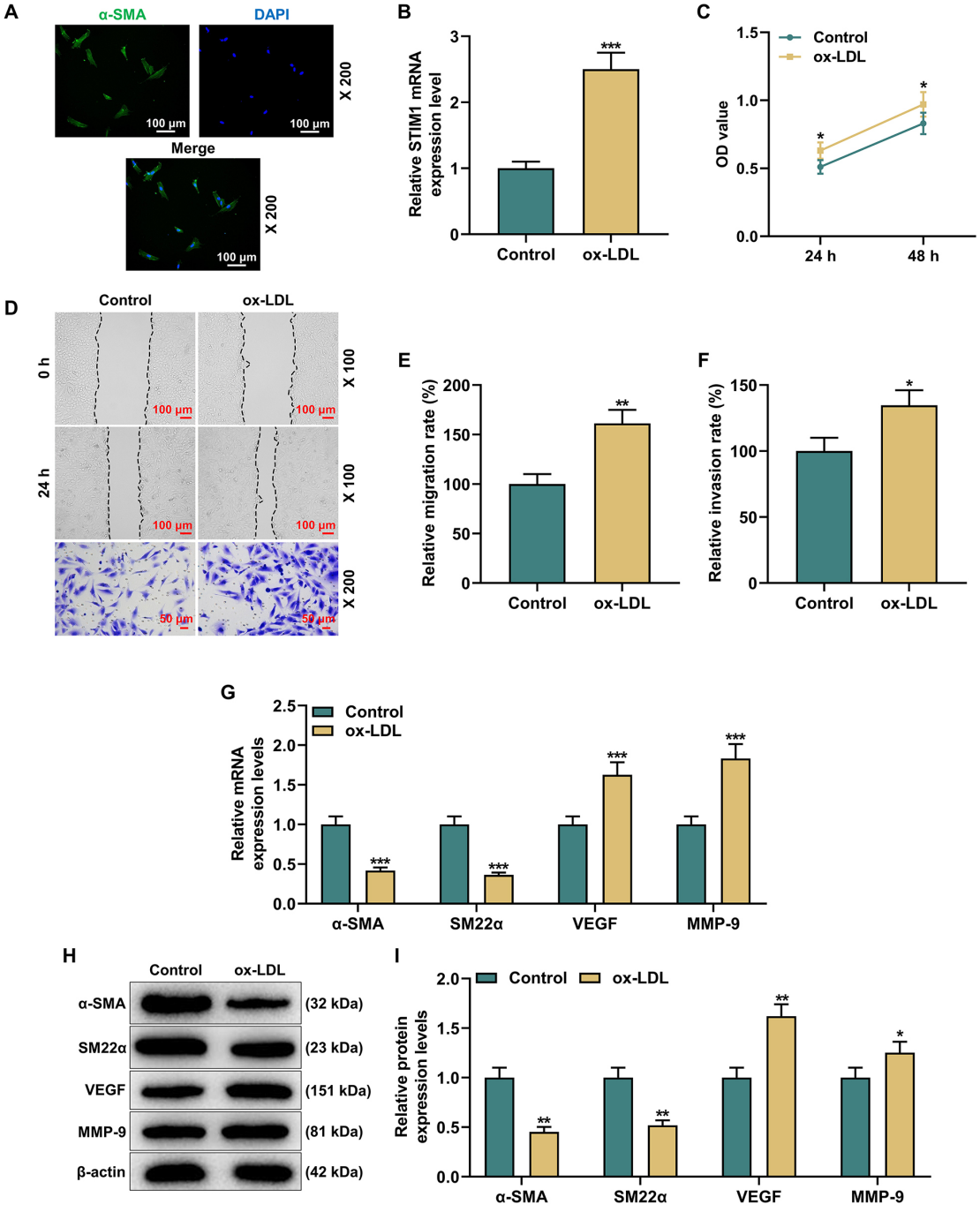

Fig. 1. Ox-LDL affected cell viability, migration, invasion, and phenotypic switching-related factors in VSMCs. (A) An immunofluorescence assay was performed to identify VSMCs. (B) Relative STIM1 expression in ox-LDL-treated VSMCs (qRT-PCR, β-actin as internal control). (C) Relative viability of ox-LDL-treated VSMCs at 24 and 48 h (CCK-8 assay). (D–F) Relative migration at 0 and 24 h (D,E) and invasion at 48 h (D,F) of ox-LDL-treated VSMCs (Scratch and Transwell assays). Magnification: $\times$100 for migration assay, $\times$200 for invasion assay. (G) The mRNA expressions of relative phenotypic switching-related factors (α-*SMA*, *SM22*α, *VEGF* and *MMP-9*) in ox-LDL-stimulated VSMCs (qRT-PCR, β-actin as internal control). (H,I) Protein expressions of relative phenotypic switching-related factors (α-SMA, SM22α, VEGF, and MMP-9) in ox-LDL-induced VSMCs (Western blotting, β-actin as internal control). All experiments were performed in triplicate and data are expressed as mean $\pm$ standard deviation (SD). $^{*}p < 0.05$, $^{**}p < 0.01$, $^{***}p < 0.001$, vs. Control. Ox-LDL, oxidized low-density lipoprotein; VSMCs, vascular smooth muscle cells; CCK-8, Cell Counting Kit-8; α-SMA, α-smooth muscle actin; SM22α, smooth muscle protein-22α; VEGF, vascular endothelial growth factor; MMP-9, matrix metalloproteinase-9; STIM1, stromal interaction molecule 1; DAPI, 4′,6-diamidino-2-phenylindole; OD, optical density.

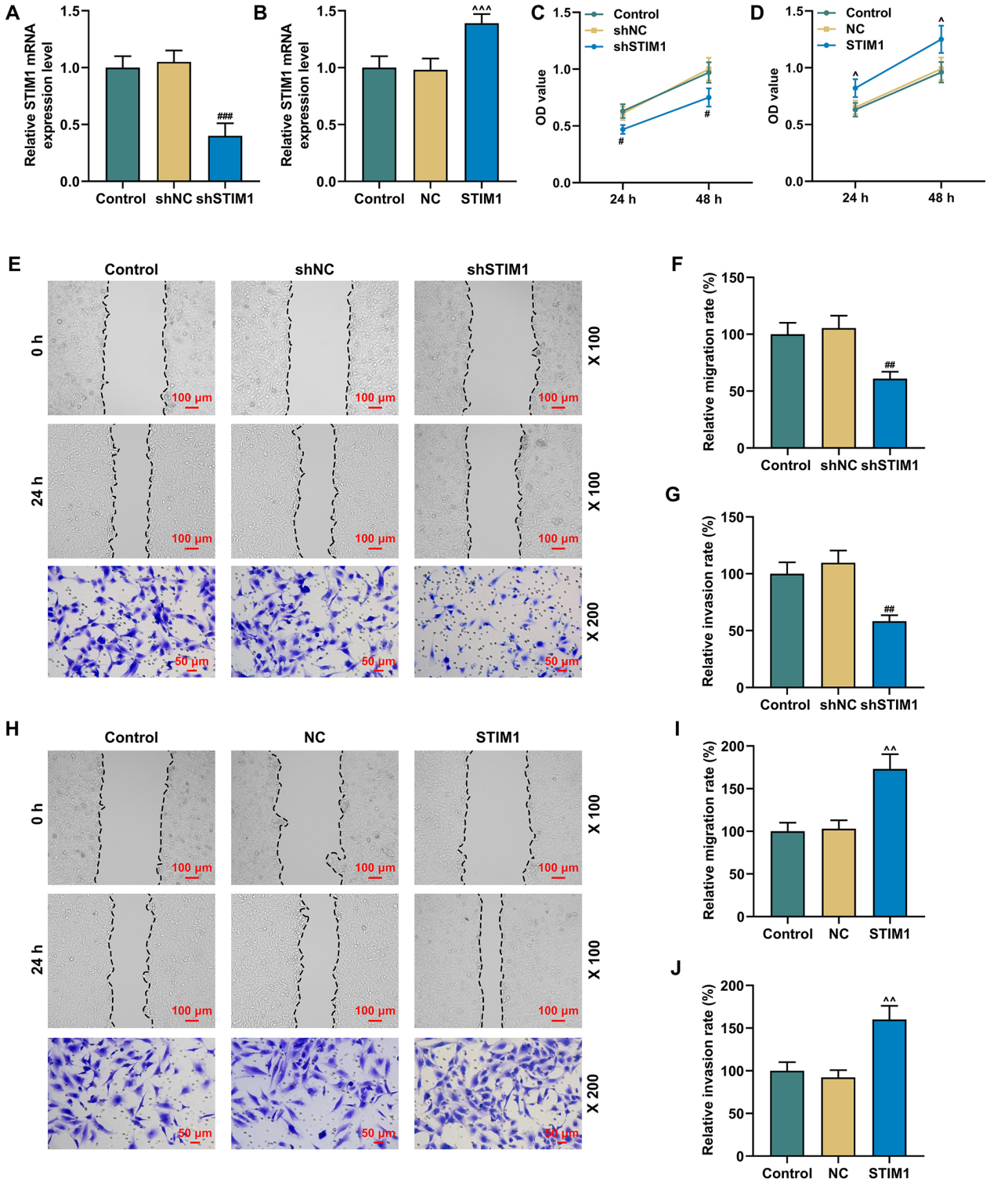

Fig. 2. STIM1 affected viability, migration, and invasion of ox-LDL-treated VSMCs. (A,B) Relative STIM1 expression following shSTIM1 (A) or STIM1 overexpression vector (B) transfection in ox-LDL-treated VSMCs (qRT-PCR, β-actin as internal control). (C,D) Viability of ox-LDL-treated VSMCs following 24/48-h shSTIM1 (C) or STIM1 overexpression vector (D) transfection (CCK-8 assay). (E–J) Migration at 0 and 24 h and invasion of ox-LDL-treated VSMCs at 48 h following shSTIM1 (E–G) or STIM1 overexpression vector (H–J) transfection (Scratch and Transwell assays). Magnification: ×100 for migration assay, ×200 for invasion assay. All experiments were performed in triplicate and data are expressed as mean ± standard deviation (SD). $^{\#}p < 0.05$, $^{\#\#}p < 0.01$, $^{\#\#\#}p < 0.001$, vs. shNC; $^{\wedge}p < 0.05$, $^{\wedge\wedge}p < 0.01$, $^{\wedge\wedge\wedge}p < 0.001$, vs. NC. shSTIM1, short hairpin RNA targeting STIM1; shNC, short hairpin RNA for negative control; NC, negative control.

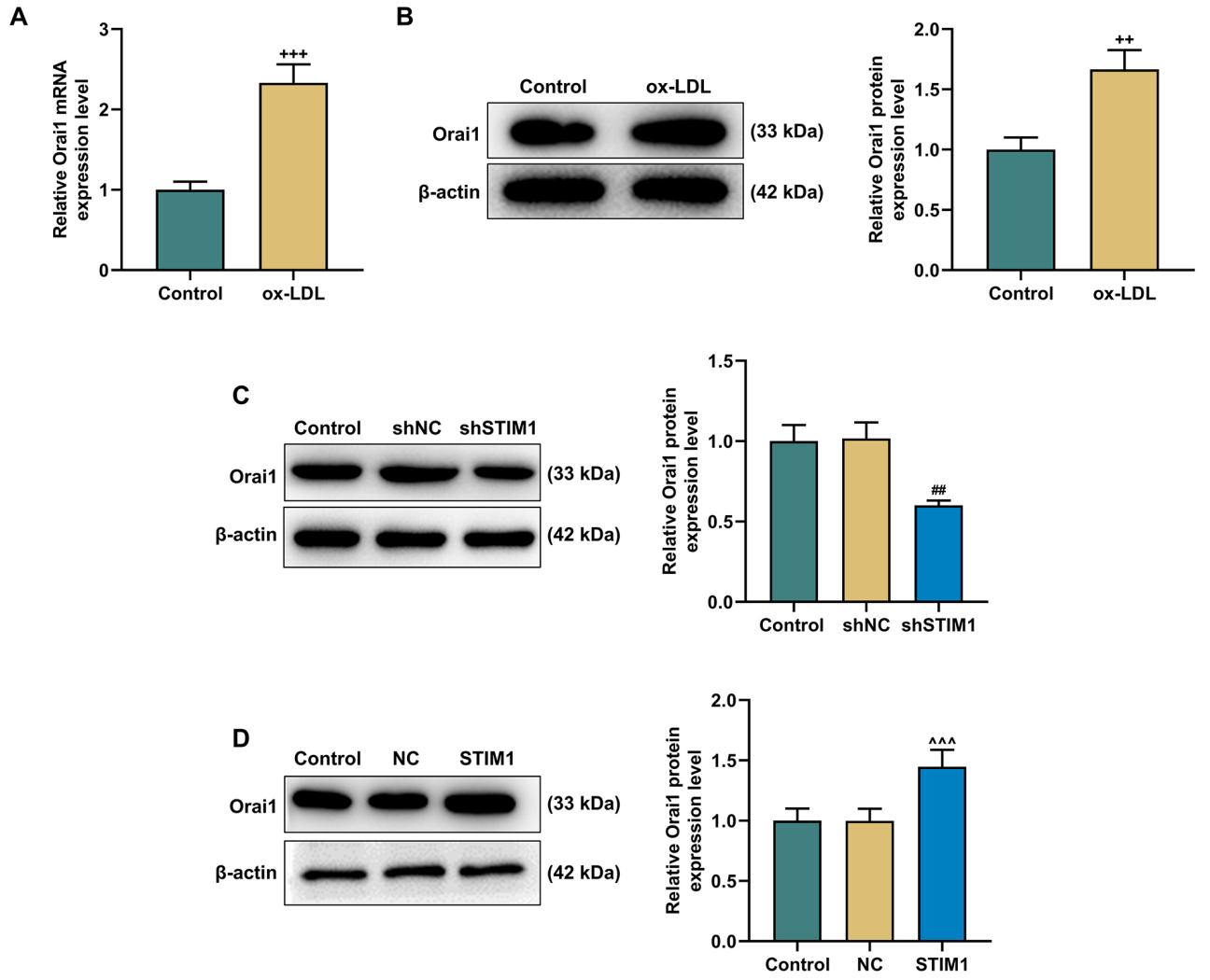

Fig. 3. Orai1 level was upregulated by ox-LDL and STIM1 overexpression yet downregulated by STIM1 silencing. (A) Relative *Orai1* mRNA expression in ox-LDL-triggered VSMCs (qRT-PCR, β-actin as internal control). (B) Relative Orai1 protein expression in ox-LDL-treated VSMCs (Western blotting, β-actin as internal control). (C,D) Relative Orai1 protein expressions in ox-LDL-treated VSMCs following shSTIM1 (C) or STIM1 overexpression vector (D) transfection (Western blotting, β-actin as internal control). All experiments were performed in triplicate and data are expressed as mean $\pm$ standard deviation (SD). $^{++}p < 0.01$, $^{+++}p < 0.001$, vs. Control; $^{\#\#}p < 0.01$, vs. shNC; $^{\wedge\wedge\wedge}p < 0.001$, vs. NC. Orai1, Orai calcium release-activated calcium modulator 1; NC, negative control.

(BCA) Protein Assay Kit (PC0020, Solarbio, China). Using sodium dodecyl sulfate-polyacrylamide gel electrophoresis (SDS-PAGE), proteins were separated in NuPAGE™ 4–12%, Bis-Tris (NP0321BOX, Invitrogen, USA), loaded onto polyvinylidene fluoride membranes (YA1701, Solarbio, China), and subjected to 1-h blocking with Blocking Buffer (37581, Invitrogen, USA) (RT). Following overnight incubation with primary antibodies against α-smooth muscle actin (α-SMA, ab108424, 1:2000, 32 kDa), smooth muscle protein-22α (SM22α, ab155272, 1:5000, 23 kDa), vascular endothelial growth factor (VEGF, ab32152, 1:5000, 151 kDa), matrix metalloproteinase-9 (MMP-9, ab228402, 1:1000, 81 kDa), Orai1 (ab175040, 1:1000, 33 kDa) and β-actin (ab8226, 1:2000, 42 kDa) (4 °C), samples were cultured for 1-h with secondary antibodies (RT), anti-rabbit IgG (ab205718, 1:2000) and anti-mouse IgG (ab205719, 1:2000) Bands were detected using a BeyoECL Plus kit (P0018S, Beyotime, Shanghai, China) and the band signal analysis was carried out on a 5200 imaging system (Tanon, Shanghai, China). All antibodies were provided from Abcam (UK). Data analysis was performed with Image J software (1.52s version, National Institutes of Health, Bethesda, MD, USA), with β-actin as the internal reference.

Statistical Analysis

All data from three independently repeated assays were expressed as mean $\pm$ standard deviation and analyzed using GraphPad Prism 8 (GraphPad, Inc., La Jolla, CA, USA). Two-group and multi-group comparisons were per-

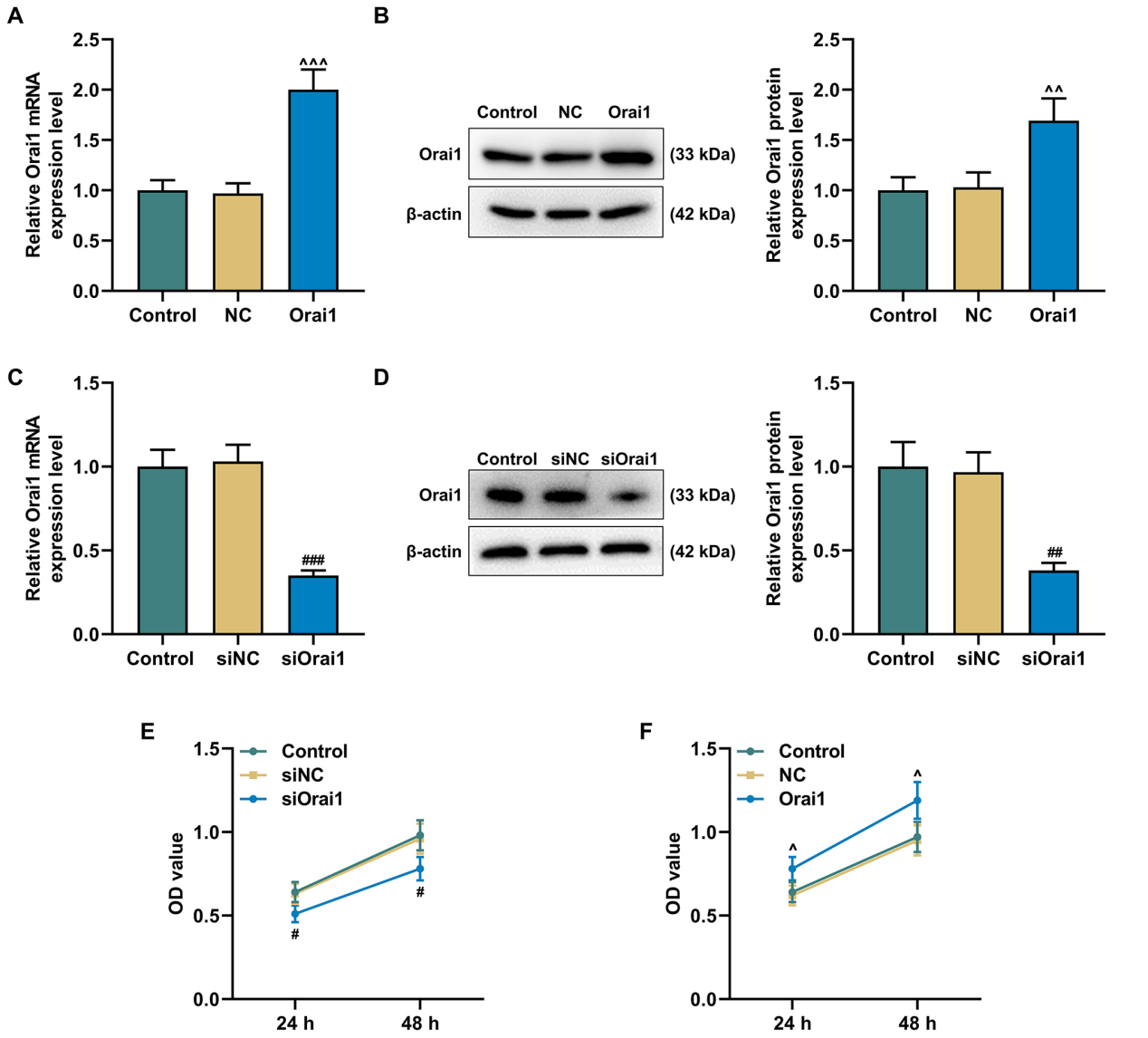

Fig. 4. Orai1 affected cell viability in ox-LDL-treated VSMCs. (A–D) Relative Orai1 expression in ox-LDL-stimulated VSMCs following Orai1 overexpression plasmid (A,B) and siOrai1 (C,D) transfection (qRT-PCR and Western blotting, β-actin as internal control). (E,F) Viability of ox-LDL-triggered VSMCs following siOrai1 (E) and Orai1 overexpression plasmid (F) transfection at 24 and 48 h (CCK-8 assay). All experiments were conducted in triplicate and data are expressed as mean ± standard deviation (SD). $^{\wedge}p < 0.05$, $^{\wedge\wedge}p < 0.01$, $^{\wedge\wedge\wedge}p < 0.001$, vs. NC; $^{\#}p < 0.05$, $^{\#\#}p < 0.01$, $^{\#\#\#}p < 0.001$, vs. siNC. siRNA, small interfering RNA; NC, negative control; siOrai1, siRNA targeting Orai1.

formed using the independent samples *t*-test and one-way ANOVA, respectively. *p*-values < 0.05 were considered statistically significant.

Results

Ox-LDL Decreased α-SMA and SM22α and Increased STIM1, VEGF, MMP-9, Viability, Migration, and Invasion in VSMCs

Immunofluorescence assay revealed that α-SMA was arranged in a muscle-like pattern along the longitudinal axis within the cytoplasm (Fig. 1A), confirming that the cells were VSMCs. We first measured STIM1 in VSMCs post ox-LDL treatment and found upregulation of STIM1 (Fig. 1B, $p < 0.001$). In addition, based on CCK-8, Scratch, and Transwell assays, ox-LDL promoted viability at 24 and 48 h, migration, and invasion in VSMCs (Fig. 1C–F, $p < 0.05$).

Since α-SMA, SM22α, VEGF, and MMP-9 have been shown to be related to phenotypic switching [22,23], their expressions were subsequently measured. Ox-LDL-treated cells displayed decreased expression of α-SMA and SM22α and increased expression of VEGF and MMP-9 (Fig. 1G–I, $p < 0.05$).

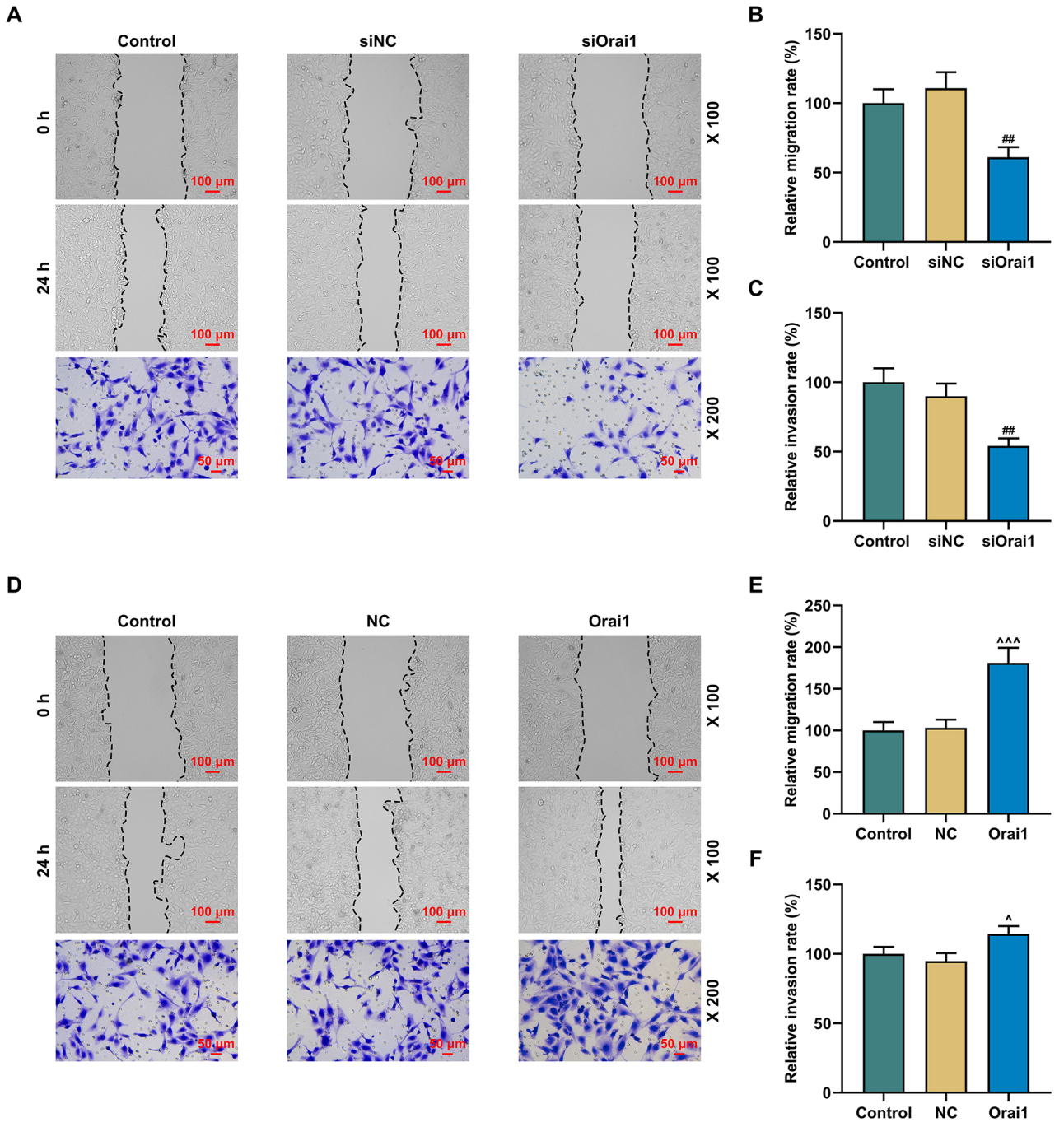

Fig. 5. Orai1 affected VSMC migration and invasion post ox-LDL stimulation. (A–F) Migration (0/24 h) and invasion (48 h) of ox-LDL-treated VSMCs following siOrai1 (A–C) and Orai1 overexpression plasmid (D–F) transfection (Scratch and Transwell assays). Magnification: ×100 for migration assay, ×200 for invasion assay. All experiments were performed in triplicate and data are expressed as mean ± standard deviation (SD). $^{\#\#}p < 0.01$, vs. siNC; $^{\wedge}p < 0.05$, $^{\wedge\wedge\wedge}p < 0.001$, vs. NC; NC, negative control.

STIM1 Downregulation Suppressed Viability, Migration, and Invasion of Ox-LDL-Triggered VSMCs, Whereas STIM1 Upregulation Had Opposite Effects

We subsequently transfected the shSTIM1 or STIM1 overexpression vector into ox-LDL-stimulated VSMCs (Fig. 2A,B, $p < 0.001$). STIM1 downregulation (Fig. 2C,E–G, $p < 0.05$) inhibited, whereas STIM1 overexpression (Fig. 2D,H–J, $p < 0.05$) promoted, viability at 24 and 48 h, migration, and invasion in ox-LDL-treated VSMCs.

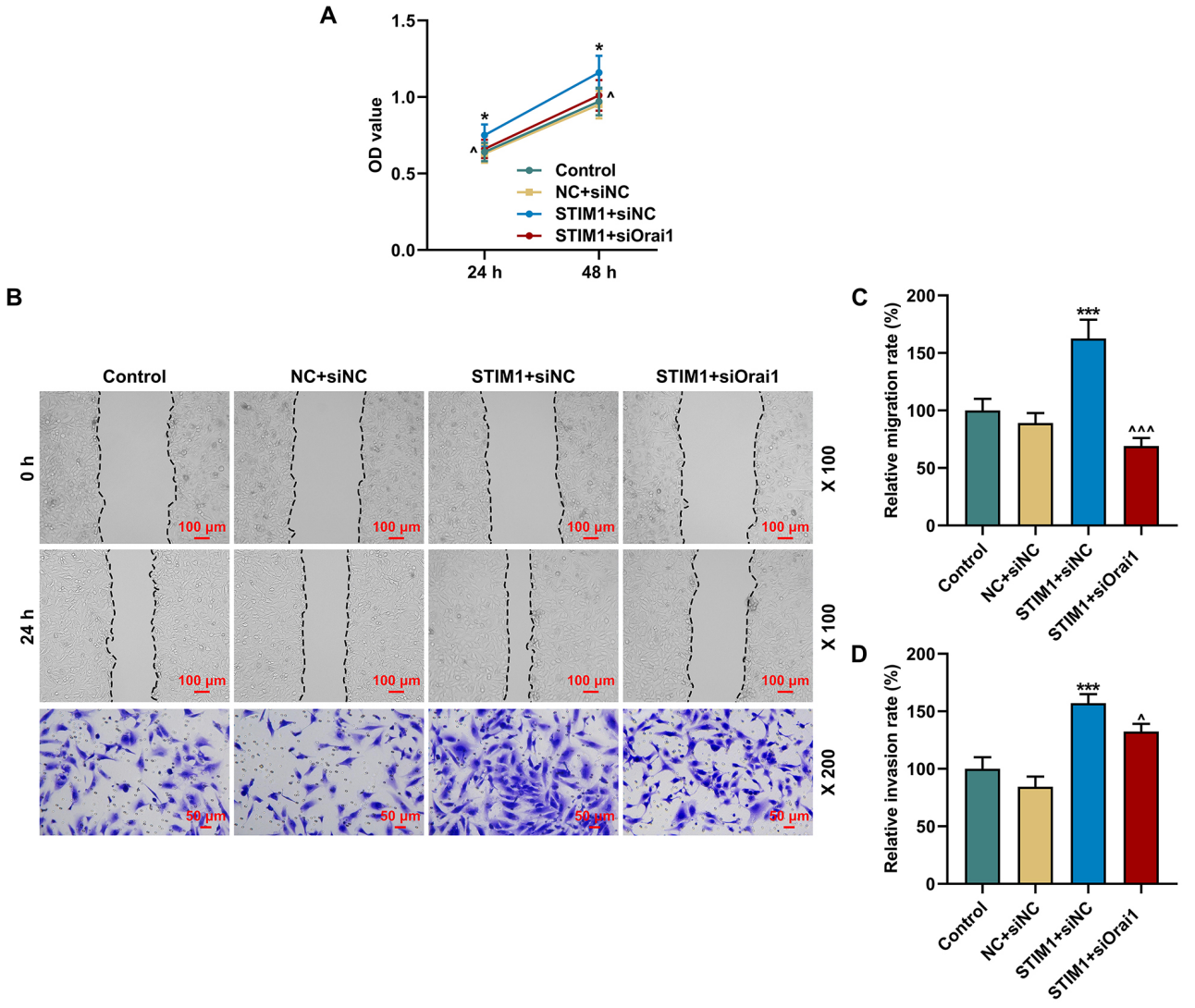

Fig. 6. Silencing of Orai1 reversed the influences of STIM1 overexpression on viability, migration and invasion in ox-LDL-treated VSMCs. (A) Viability of ox-LDL-stimulated VSMCs following STIM1 overexpression plasmid and siOrai1 transfection at 24/48 h (CCK-8 assay). (B–D) Migration (0/24 h) and invasion (48 h) of ox-LDL-treated VSMCs following STIM1 overexpression plasmid and siOrai1 transfection (Scratch and Transwell assays). Magnification: ×100 for migration assay, ×200 for invasion assay. All experiments were performed in triplicate and data are expressed as mean ± standard deviation (SD). $^{*}p < 0.05$, $^{***}p < 0.001$, vs. NC+siNC; $^{\wedge}p < 0.05$, $^{\wedge\wedge\wedge}p < 0.001$, vs. STIM1+siNC; NC, negative control.

Orai1 Level was Upregulated by Ox-LDL and STIM1 Overexpression yet Downregulated by STIM1 Silencing

To gauge the influence of Orai1 on VSMCs, Orai1 expression was measured in VSMCs with/without ox-LDL treatment, and upregulation of Orai1 was discovered in ox-LDL-stimulated VSMCs (Fig. 3A,B, $p < 0.01$). In addition, following STIM1 downregulation, the Orai1 level in model cells was decreased, whereas STIM1 upregulation further promoted Orai1 expression (Fig. 3C,D, $p < 0.01$).

Orai1 Deficiency Suppressed Viability, Migration, and Invasion in Ox-LDL-Induced VSMCs, Whereas Orai1 Overexpression Had Opposite Effects

To detect the role of Orai1 in ox-LDL-stimulated VSMCs, Orai1 overexpression plasmid and siOrai1 were transfected into model cells (Fig. 4A–D, $p < 0.01$). CCK-8 assay results at 24 and 48 h revealed that Orai1 silencing suppressed, yet Orai1 overexpression promoted, model cell viability (Fig. 4E,F, $p < 0.05$). Next, the effects of Orai1 silencing or overexpression on migration and invasion of model cells were assessed using Scratch and Transwell assays. Depletion of Orai1 suppressed (Fig. 5A–C, $p < 0.01$), whereas Orai1 overexpression enhanced, migration and invasion of model cells (Fig. 5D–F, $p < 0.05$).

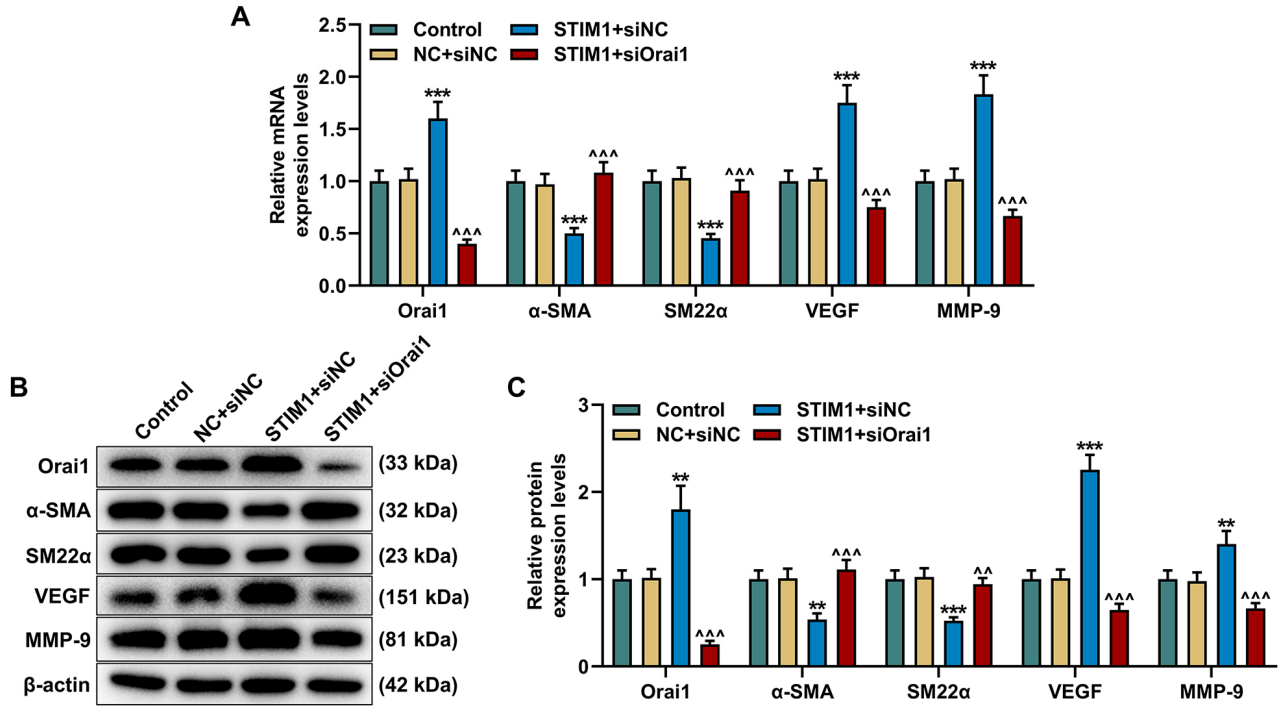

Fig. 7. Orai1 silencing reversed the influences of STIM1 overexpression on Orai1 and phenotypic switching-related factor expression in ox-LDL-stimulated VSMCs. (A) Orai1 and phenotypic switching-related factor expression in ox-LDL-treated VSMCs following STIM1 overexpression plasmid and siOrai1 transfection (qRT-PCR, β-actin as internal control). (B,C) Orai1 and phenotypic switching-related factor expression in ox-LDL-stimulated VSMCs following STIM1 overexpression plasmid and siOrai1 transfection (Western blotting, β-actin as internal control). All experiments were performed in triplicate and data are expressed as mean $\pm$ standard deviation (SD). $^{**}p < 0.01$, $^{***}p < 0.001$, vs. NC+siNC; $^{\wedge\wedge}p < 0.01$, $^{\wedge\wedge\wedge}p < 0.001$, vs. STIM1+siNC; NC, negative control.

Orai1 Silencing Reversed the Influences of STIM1 Overexpression on Viability, Migration, Invasion, and Expression of Orai1 and Phenotypic Switching-Related Factors in Ox-LDL-Treated VSMCs

To detect the effects of interaction between STIM1 and Orai1, STIM1 overexpression vectors and siOrai1 were transfected into ox-LDL-treated VSMCs, and it was discovered that STIM1 overexpression promoted viability at 24 and 48 h (Fig. 6A, $p < 0.05$), migration, and invasion in model cells (Fig. 6B–D, $p < 0.001$), the effects of which were attenuated by silencing of Orai1 (Fig. 6A–D, $p < 0.05$).

Through qRT-PCR and Western blotting, we analyzed the effects of STIM1 and Orai1 on the expression of Orai1 and phenotypic switching-related factors. We found that after STIM1 overexpression, Orai1, VEGF, and MMP-9 expressions were increased, whereas α-SMA and SM22α expressions were decreased (Fig. 7A–C, $p < 0.01$); however, silencing of Orai1 counteracted the influences of STIM1 overexpression on Orai1 and phenotypic switching-related factor expression (Fig. 7A–C, $p < 0.01$).

STIM1 Silencing Alleviated AS and Regulated Orai1 and Phenotypic Switching-Related Factor Expression in Vivo

Finally, we constructed an AS model *in vivo* to further determine the effects of STIM1 *in vivo*. According to the results of H&E staining, no aortic atheromatous plaque formation and no evident change in interlayer VSMCs were found in mice of the Control group, whereas aortic atheromatous plaque formation and reduced VSMCs were evidenced in AS model mice with or without shSTIM1 injection (Fig. 8A). In mice of the Model+shSTIM1 group, we detected reduced aortic atheromatous plaque and arranged VSMCs in the aorta, denoting ameliorative effects (Fig. 8A). These results suggested that silencing STIM1 may have an alleviating effect on the AS model *in vivo*.

Also, results from IHC analysis suggested that the number of STIM1-positive aortic VSMCs was increased following AS model construction, whereas it was reduced by shSTIM1 (Fig. 8B,C, $p < 0.001$). In addition, results from qRT-PCR and Western blotting indicated that in smooth muscle tissue, following AS model construction, Orai1, VEGF, and MMP-9 expressions were increased, whereas those of α-SMA and SM22α were decreased (Fig. 8D–F, $p < 0.001$). However, silencing of STIM1 downregulated Orai1, VEGF, and MMP-9 levels and up-

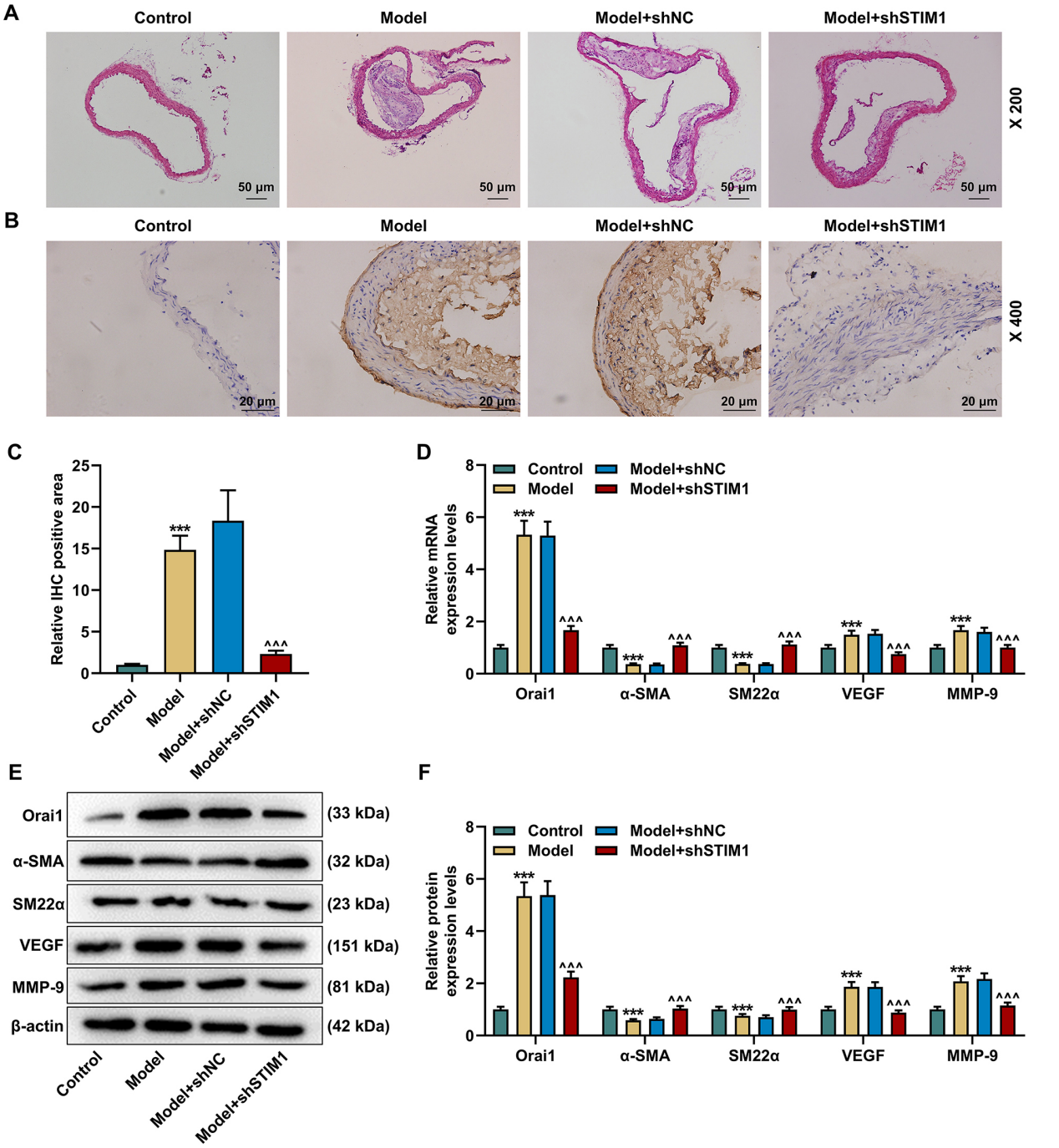

Fig. 8. STIM1 silencing alleviated AS and regulated Orai1 and phenotypic switching-related factor expression *in vivo*. (A) Aortic sample detection after AS model construction and treatment (H&E staining, ×200 magnification). (B,C) STIM1 level in aortic sample after AS model construction and treatment (immunohistochemistry analysis, ×400 magnification). (D) Relative mRNA expressions of Orai1 and phenotypic switching-related factors (α-SMA; SM22α; VEGF, and MMP-9) (qRT-PCR, β-actin as internal control). (E,F) Relative protein expression of Orai1 and phenotypic switching-related factors (α-SMA; SM22α; VEGF and MMP-9) (Western blotting, β-actin as internal control). All experiments were performed in triplicate and data are expressed as mean ± standard deviation (SD). $^{***}p < 0.001$, vs. Control; $^{\wedge\wedge\wedge}p < 0.001$, vs. Model+shNC. AS, atherosclerosis; H&E, hematoxylin-eosin.

regulated those of α-SMA and SM22α in the AS model (Fig. 8D–F, $p < 0.001$). These results revealed that silencing of STIM1 could regulate the expressions of Orai1 and phenotypic switching-related factors *in vivo*.

Discussion

AS, a common CVD in which fatty and/or fibrous materials accumulate within the innermost aortic areas, im-

pacts morbidity and mortality all over the world [4]. In our study, we investigated the role of STIM1 in AS based on an *in vitro* model using ox-LDL-treated VSMCs and an *in vivo* model with high-fat diet-treated mice. Finally, we discovered that STIM1 downregulation suppressed viability, migration and invasion of ox-LDL-treated cells, mediated expressions of phenotypic switching-related factors *in vitro*, and ameliorated AS *in vivo*.

Increasing evidence has suggested a role for VSMCs in AS. Specifically, VSMCs are dominant cells in arterial walls and change both functionally and structurally in response to atherogenic factors; moreover, improving the function of VSMCs can help decelerate AS development to some extent [24]. Under stimulation of some cytokines, growth factors, or Ang II, VSMCs may proliferate and migrate, which is instrumental in AS pathogenesis [25]. Also, in normal arteries, VSMCs tend to be quiescent, with a contractile phenotype related to the stable production of specific proteins such as α-SMA and SM22α [26]. Encoded by actin α2, α-SMA is a vascular smooth muscle actin isoform, expressed in VSMCs, that induces the motility and contraction of the vascular wall. SM22α, an actin-binding protein, enhances VSMC contractility and mobility, and its activation contributes to balancing the differentiated phenotype in VSMCs [27]. Triggered by both inflammation and injury, VSMCs may undergo the process of phenotypic switching from a contractile phenotype to an adverse proliferative one, which is a hallmark of the development of vascular pathologies, including AS [28]. VEGF has been found to diminish the promoting effects of Myocardin on contractile markers, whereas MMP-9 is one of the extracellular matrix components in synthetic VSMCs [29,30]. In this study, we demonstrated that ox-LDL treatment boosted viability, migration, invasion, and phenotypic switching of VSMCs, and was associated with upregulation of VEGF and MMP-9 expression and downregulation of α-SMA and SM22α expression.

STIM1, a member of the class of STIM proteins that are Ca^{2+}-sensing coordinators, is one of the multidomain, single-pass proteins with transmembrane capability implicated in sensing changes within compartmentalized Ca^{2+} levels and cellular signal transduction to Orai channel proteins [31,32]. Tropomyosin 3 interacts with STIM1 to regulate vascular smooth muscle contractility, thereby leading to hypertension [33]. Also, multiple non-coding RNAs can regulate STIM1 expression and then cause VSMCs to proliferate, migrate, and invade [12,34,35]. Here, we found that STIM1 downregulation attenuates the influence of ox-LDL on VSMCs, which also suppresses cell viability, migration, and invasion *in vitro* and alleviates AS *in vivo*. These results provide new evidence on the role of STIM1 in ox-LDL-stimulated VSMCs and AS. Nevertheless, the detailed molecular mechanism awaits to be further clarified.

The previous study have revealed a distinct STIM-Orai activating region (SOAR1) inside discrete ER-plasma membrane (PM) junctions when STIM1 protein dimers unfold, resulting in the tethering and activation of Orai1 channels [36]. STIM1 and Orai1 are highly expressed in injured arteries, and this may be related to VSMC proliferation in vascular remodeling [37]. In our study, we confirmed that Orai1 level was upregulated by ox-LDL and STIM1 overexpression, and silencing of Orai1 suppressed viability, migration, and invasion of ox-LDL-treated VSMCs, whereas Orai1 overexpression has opposite effects. Moreover, Orai1 deficiency reversed the effects of STIM1 overexpression in ox-LDL-treated VSMCs *in vitro*, indicating that the influences of STIM1 on ox-LDL-treated VSMCs are possibly achieved via targeting Orai1.

Conclusion

To sum up, we found evidence that STIM1 activates Orai1 to regulate phenotypic switching of VSMCs, thereby participating in plaque instability of AMI. We hope that our work will contribute to a better understanding of the possible preventative treatments for AS.

Availability of Data and Materials

The datasets used and analyzed during the current study are available from the corresponding author upon reasonable request.

Author Contributions

Substantial contributions to conception and design: ZYC, YZ; Data acquisition, data analysis and interpretation: LZS; Drafting the article or critically revising it for important intellectual content: ZYC, YZ, LZS; Final approval of the version to be published: ZYC, YZ, LZS; Agreement to be accountable for all aspects of the work in ensuring that questions related to the accuracy or integrity of the work are appropriately investigated and resolved: ZYC, YZ, LZS.

Ethics Approval and Consent to Participate

The animal experiment was approved by the Ethics Committee of Zhejiang Baiyue Biotech Co., Ltd. for Experimental Animal Welfare (approval number: ZJBYLA-IACUC-20230427). In addition to approval from the Ethics Committee for this study, all animal studies also followed the guidelines of the China Council on Animal Care and Use.

Acknowledgment

Not applicable.

Funding

This research received no external funding.

Conflict of Interest

The authors declare no conflict of interest.

References

[1] Xu H, Jiang J, Chen W, Li W, Chen Z. Vascular Macrophages in Atherosclerosis. Journal of Immunology Research. 2019; 2019: 4354786.

[2] Ding Y, Liu N, Zhang D, Guo L, Shang Q, Liu Y, *et al*. Mitochondria-associated endoplasmic reticulum membranes as a therapeutic target for cardiovascular diseases. Frontiers in Pharmacology. 2024; 15: 1398381.

[3] In China TWCOTROCHAD, Hu SS. Report on cardiovascular health and diseases in China 2021: an updated summary. Journal of Geriatric Cardiology: JGC. 2023; 20: 399–430.

[4] Fan J, Watanabe T. Atherosclerosis: Known and unknown. Pathology International. 2022; 72: 151–160.

[5] Dong Z, Hou L, Luo W, Pan LH, Li X, Tan HP, *et al*. Myocardial infarction drives trained immunity of monocytes, accelerating atherosclerosis. European Heart Journal. 2024; 45: 669–684.

[6] Sun C, Fu Y, Gu X, Xi X, Peng X, Wang C, *et al*. Macrophage-Enriched lncRNA RAPIA: A Novel Therapeutic Target for Atherosclerosis. Arteriosclerosis, Thrombosis, and Vascular Biology. 2020; 40: 1464–1478.

[7] Silvério de Barros R, Dias GS, Paula do Rosario A, Paladino FV, Lopes GH, Campos AH. Gremlin-1 potentiates the dedifferentiation of VSMC in early stages of atherosclerosis. Differentiation; Research in Biological Diversity. 2019; 109: 28–33.

[8] Basatemur GL, Jørgensen HF, Clarke MCH, Bennett MR, Mallat Z. Vascular smooth muscle cells in atherosclerosis. Nature Reviews. Cardiology. 2019; 16: 727–744.

[9] Johnson MT, Gudlur A, Zhang X, Xin P, Emrich SM, Yoast RE, *et al*. L-type Ca^{2+} channel blockers promote vascular remodeling through activation of STIM proteins. Proceedings of the National Academy of Sciences of the United States of America. 2020; 117: 17369–17380.

[10] Tanwar J, Trebak M, Motiani RK. Cardiovascular and Hemostatic Disorders: Role of STIM and Orai Proteins in Vascular Disorders. Advances in Experimental Medicine and Biology. 2017; 993: 425–452.

[11] Saint Fleur-Lominy S, Maus M, Vaeth M, Lange I, Zee I, Suh D, *et al*. STIM1 and STIM2 Mediate Cancer-Induced Inflammation in T Cell Acute Lymphoblastic Leukemia. Cell Reports. 2018; 24: 3045–3060.e5.

[12] Lv Z, Yi D, Zhang C, Xie Y, Huang H, Fan Z, *et al*. miR 541 3p inhibits the viability and migration of vascular smooth muscle cells via targeting STIM1. Molecular Medicine Reports. 2021; 23: 312.

[13] Lunz V, Romanin C, Frischauf I. STIM1 activation of Orai1. Cell Calcium. 2019; 77: 29–38.

[14] Shrestha N, Bacsa B, Ong HL, Scheruebel S, Bischof H, Malli R, *et al*. TRIC-A shapes oscillatory Ca2+ signals by interaction with STIM1/Orai1 complexes. PLoS Biology. 2020; 18: e3000700.

[15] Liu B, Zhang B, Roos CM, Zeng W, Zhang H, Guo R. Upregulation of Orai1 and increased calcium entry contribute to angiotensin II-induced human coronary smooth muscle cell proliferation: Running Title: Angiotensin II-induced human coronary smooth muscle cells proliferation. Peptides. 2020; 133: 170386.

[16] Shawer H, Norman K, Cheng CW, Foster R, Beech DJ, Bailey MA. ORAI1 Ca^{2+} Channel as a Therapeutic Target in Pathological Vascular Remodelling. Frontiers in Cell and Developmental Biology. 2021; 9: 653812.

[17] Kattoor AJ, Kanuri SH, Mehta JL. Role of Ox-LDL and LOX-1 in Atherogenesis. Current Medicinal Chemistry. 2019; 26: 1693–1700.

[18] Wu X, Zheng X, Cheng J, Zhang K, Ma C. LncRNA TUG1 regulates proliferation and apoptosis by regulating miR-148b/IGF2 axis in ox-LDL-stimulated VSMC and HUVEC. Life Sciences. 2020; 243: 117287.

[19] Cheng S, Zhou F, Xu Y, Liu X, Zhang Y, Gu M, *et al*. Geniposide regulates the miR-101/MKP-1/p38 pathway and alleviates atherosclerosis inflammatory injury in $ApoE^{-/-}$ mice. Immunobiology. 2019; 224: 296–306.

[20] Estrada-Luna D, Martínez-Hinojosa E, Cancino-Diaz JC, Belefant-Miller H, López-Rodríguez G, Betanzos-Cabrera G. Daily supplementation with fresh pomegranate juice increases paraoxonase 1 expression and activity in mice fed a high-fat diet. European Journal of Nutrition. 2018; 57: 383–389.

[21] Livak KJ, Schmittgen TD. Analysis of relative gene expression data using real-time quantitative PCR and the 2(-Delta Delta C(T)) Method. Methods (San Diego, Calif.). 2001; 25: 402–408.

[22] Burger F, Baptista D, Roth A, da Silva RF, Montecucco F, Mach F, *et al*. NLRP3 Inflammasome Activation Controls Vascular Smooth Muscle Cells Phenotypic Switch in Atherosclerosis. International Journal of Molecular Sciences. 2021; 23: 340.

[23] Wang X, Li D, Chen H, Wei X, Xu X. Expression of Long Noncoding RNA LIPCAR Promotes Cell Proliferation, Cell Migration, and Change in Phenotype of Vascular Smooth Muscle Cells. Medical Science Monitor: International Medical Journal of Experimental and Clinical Research. 2019; 25: 7645–7651.

[24] Miano JM, Fisher EA, Majesky MW. Fate and State of Vascular Smooth Muscle Cells in Atherosclerosis. Circulation. 2021; 143: 2110–2116.

[25] Grootaert MOJ, Bennett MR. Vascular smooth muscle cells in atherosclerosis: time for a re-assessment. Cardiovascular Research. 2021; 117: 2326–2339.

[26] Zhang F, Guo X, Xia Y, Mao L. An update on the phenotypic switching of vascular smooth muscle cells in the pathogenesis of atherosclerosis. Cellular and Molecular Life Sciences: CMLS. 2021; 79: 6.

[27] Shen X, Xie X, Wu Q, Shi F, Chen Y, Yuan S, *et al*. S-adenosylmethionine attenuates angiotensin II-induced aortic dissection formation by inhibiting vascular smooth muscle cell phenotypic switch and autophagy. Biochemical Pharmacology. 2024; 219: 115967.

[28] Tang HY, Chen AQ, Zhang H, Gao XF, Kong XQ, Zhang JJ. Vascular Smooth Muscle Cells Phenotypic Switching in Cardiovascular Diseases. Cells. 2022; 11: 4060.

[29] Liao XH, Xiang Y, Li H, Zheng DL, Xu Y, Xi Yu C, *et al*. VEGF-A Stimulates STAT3 Activity via Nitrosylation of Myocardin to Regulate the Expression of Vascular Smooth Muscle Cell Differentiation Markers. Scientific Reports. 2017; 7: 2660.

[30] Huang B, Niu Y, Chen Z, Yang Y, Wang X. Integrin $\alpha 9$ is involved in the pathopoiesis of acute aortic dissection via mediating phenotype switch of vascular smooth muscle cell. Biochemical and Biophysical Research Communications. 2020; 533: 519–525.

[31] Mancarella S, Potireddy S, Wang Y, Gao H, Gandhirajan RK, Autieri M, *et al*. Targeted STIM deletion impairs calcium homeostasis, NFAT activation, and growth of smooth muscle. FASEB Journal: Official Publication of the Federation of American Societies for Experimental Biology. 2013; 27: 893–906.

[32] Novello MJ, Zhu J, Feng Q, Ikura M, Stathopulos PB. Structural elements of stromal interaction molecule function. Cell Calcium. 2018; 73: 88–94.

[33] Xu F, Zhu J, Chen Y, He K, Guo J, Bai S, *et al*. Physical interaction of tropomyosin 3 and STIM1 regulates vascular smooth muscle contractility and contributes to hypertension. Biomedicine & Pharmacotherapy = Biomedecine & Pharmacotherapie. 2021; 134: 111126.

[34] Huang Z, Li P, Wu L, Zhang D, Du B, Liang C, *et al*.

Hsa_circ_0029589 knockdown inhibits the proliferation, migration and invasion of vascular smooth muscle cells via regulating miR-214-3p and STIM1. Life Sciences. 2020; 259: 118251.

[35] Mao YY, Wang JQ, Guo XX, Bi Y, Wang CX. Circ-SATB2 upregulates STIM1 expression and regulates vascular smooth muscle cell proliferation and differentiation through miR-939. Biochemical and Biophysical Research Communications. 2018; 505: 119–125.

[36] Zhou Y, Nwokonko RM, Cai X, Loktionova NA, Abdulqadir R, Xin P, *et al*. Cross-linking of Orai1 channels by STIM proteins. Proceedings of the National Academy of Sciences of the United States of America. 2018; 115: E3398–E3407.

[37] Martín-Bórnez M, Ávila-Medina J, Calderón-Sánchez E, Rosado JA, Ordoñez-Fernández A, Smani T. Essential role of Orai1 and SARAF in vascular remodeling: Calcium Signaling and Excitation–Contraction in Cardiac, Skeletal and Smooth Muscle. Journal of General Physiology. 2021; 154: e2021ecc19.